

Secondary analysis: Graph analysis of brain connectivity network in autism spectrum disorder

Fatemeh Pourmoghari¹, Nasrin Borumandnia², Seyyed Mohammad Tabatabaei³, Hamid Alavimajd⁴

¹Department of Community Medicine, Faculty of Medicine, Dezful University of Medical Sciences, Dezful, Iran, ²Urology and Nephrology Research Centre, Shahid Beheshti University of Medical Sciences, Tehran, Iran, ³Department of Medical Informatics, Faculty of Medicine, Mashhad University of Medical Sciences, Mashhad, Iran, ⁴Department of Biostatistics, Faculty of Paramedical Sciences, Shahid Beheshti University of Medical Sciences, Tehran, Iran

Background: Autism spectrum disorder is a neurodevelopmental condition in which impaired connectivity of the brain network. The functional magnetic resonance imaging (fMRI) technique can provide information on the early diagnosis of autism by evaluating communication patterns in the brain. The present study aimed to assess functional connectivity (FC) variations in autism patients. **Materials and Methods:** Resting-state fMRI data were obtained from the "ABIDE" website. These data include 294 autism patients with a mean (standard deviation) age of 16.49 (7.63) and 312 healthy individuals with a mean (standard deviation) age of 15.98 (6.31). In this study, changes in communication patterns across different brain regions in autism patients were investigated using graph-based models. **Results:** The FC cluster of 17 regions in the brain, such as the hippocampus, cuneus, and inferior temporal, was different between the patient and healthy groups. Based on connectivity analysis of pair regions, 36 of the 136 correlations in the cluster were significantly different between the two groups. The middle temporal gyrus had more communication than the other regions. The largest difference between groups was -0.112 , which corresponding to the right middle temporal and right thalamus regions. **Conclusion:** The findings of this study revealed functional relationship alterations in patients with autism compared to healthy individuals, indicating the disease's effects on the brain connectivity network.

Key words: Autism spectrum disorder, brain connectome, functional magnetic resonance imaging

How to cite this article: Pourmoghari F, Borumandnia N, Tabatabaei SM, Alavimajd H. Secondary analysis: Graph analysis of brain connectivity network in autism spectrum disorder. *J Res Med Sci* 2024;29:2.

INTRODUCTION

Autism spectrum disorder (ASD) is a neurodevelopmental disease that begins in early childhood and lasts into adulthood. The total prevalence of ASD was 16.8/1000 children aged 8 years in 2014, and the rate has risen rapidly in recent decades. Estimates of ASD prevalence differed by gender, with males being four times more likely than females to be diagnosed with the disorder.^[1] ASD is frequently characterized by a number of mental development disorders, including impaired cognitive, intellectual, social interaction, and language abilities.^[2]

Resting-state functional magnetic resonance imaging (rs-fMRI) is a noninvasive tool that can provide

information on functional connectivity (FC) alterations in the brain by measuring blood-oxygen-level-dependent signals. FC studies can identify biomarkers for ASD diagnoses by examining correlations between different regions of the brain.^[3,4] Early ASD diagnosis and intervention planning can lead to fewer problematic behaviors and a better quality of life for patients.^[5,6] As a result, selecting the appropriate FC model is essential for effectively diagnosing ASD.

Group-level FC analyses are usually performed based on graph theory in the form of nodes and edges in which the brain regions and the correlation between them are represented by nodes and edges, respectively.^[7-9] In these methods, the correlations across the brain areas are

Access this article online

Quick Response Code:



Website:

<https://journals.lww.com/jrms>

DOI:

10.4103/jrms.jrms_428_22

This is an open access journal, and articles are distributed under the terms of the Creative Commons Attribution-NonCommercial-ShareAlike 4.0 License, which allows others to remix, tweak, and build upon the work non-commercially, as long as appropriate credit is given and the new creations are licensed under the identical terms.

For reprints contact: WKHLRPMedknow_reprints@wolterskluwer.com

Address for correspondence: Prof. Hamid Alavimajd, Faculty of Paramedical Sciences, Shahid Beheshti University of Medical Sciences, Darband St., Ghods Sq., Tehran 19716-53313, Iran.

E-mail: alavimajd@sbmu.ac.ir; alavimajd@gmail.com

Submitted: 13-Jun-2022; **Revised:** 15-Jul-2023; **Accepted:** 21-Sep-2023; **Published:** 30-Jan-2024

calculated, and then the hypothesis of equal connectivity structure between healthy and patient groups are assessed using a statistical test. However, due to a large number of correlation parameters, subject heterogeneity, and temporal autocorrelation of the data, assessing FC data is usually problematic. Accordingly, the advanced models based on the graph theory introduced by Wu *et al.* and Fiecas *et al.* were employed in this study to evaluate the brain connectivity network of autism patients, taking into account the characteristics of FC data.^[10,11]

MATERIALS AND METHODS

Subjects

The data of this study were downloaded from the publicly available ABIDE website at http://fcon_1000.projects.nitrc.org/indi/abide/.^[12] The details of inclusion and exclusion criteria are explained on the ABIDE website at http://fcon_1000.projects.nitrc.org/indi/abide/abide_I.html. This study was approved by the Ethics Committee of Shahid Beheshti University of Medical Sciences (IR. SBMU. RETECH. REC.1399.820). According to the AAI atlas, the 90 regions were extracted and considered in the analysis.^[13] ABIDE includes structural and rs-fMRI data collected from 17 international imaging sites. Data from ABIDE were preprocessed by different methods, including the usage (or not) of filtering and global signal correction. Structural preprocessing was performed using different pipelines: ANTS, CIVET, and FreeSurfer. The detailed scan processes and protocols are described on the ABIDE website at <http://preprocessed-connectomes-project.org/abide/>.

Statistical analysis

Adaptive dense subgraph discovery (ADSD) and variance component models were used to compare the brain connectivity of autistic patients to the healthy group.^[10,11] The ADSD model is determined to identify a disease-related cluster of regions, and then the variance component model is applied to compare the pairwise connectivity of the selected regions.

In the ADSD model, $G = (V, E, W)$ represents a graph that consists of V nodes or desired regions, $E = V(V-1)/2$ edges, and an adjacency matrix W . The adjacency matrix contains information about the edgewise inference findings. $G(S) = (S, E(S))$ is defined as a cluster of G with $S \subset V$, and $E(S) = \{(u, v) \in E \mid u, v \in S\}$. The following is an adaptive density function:

$$f(S, \lambda) = \frac{|W(S)|}{|S|^2} \quad (1)$$

Where λ is used as a tuning parameter, finally, an iterative algorithm is used to optimize Eq. (1) and the estimation of λ .

The variance component model is defined as follows to evaluate the FC among the selected regions as pairwise:

$$Y = X\beta + \varepsilon + \psi \quad (2)$$

The vector Y represents the correlation coefficient between the selected regions, obtained by the ADSD model. Let X be the design matrix, and β indicates the estimation of edge parameters. The error terms ε and ψ capture the variation between edges and the subject heterogeneity, respectively.

The following test statistics are employed by the permutation approach to compare the FC of regions between the patient and healthy groups:

$$\left(C(\beta_1 - \beta_2) \right)' \left(C(\text{var}(\beta_1) + \text{var}(\beta_2))C' \right)^{-1} \left(C(\beta_1 - \beta_2) \right), \quad (3)$$

Where C is an identity matrix. The vectors β_1 and β_2 represent estimates of each group's edges parameters. In order to adjust the P values Eq. (3), the FDR (false discovery rate) is used to correct multiple comparisons. In this study, 1000 permutations were considered for the statistical test. The data analysis was performed with R software version 4.0.5 and MATLAB R2019b.

The Mann–Whitney nonparametric test was used to compare age and full intelligence quotient score variables between the patient and healthy groups.

RESULTS

The rs-fMRI data included 294 men with autism and 312 healthy men. There was no significant difference in age ($P = 0.672$) and full intelligence quotient score ($P = 0.663$) distributions between the two groups [Table 1]. The first ADSD model was applied on 90 regions, which were extracted based on the AAI atlas. A cluster of 17 regions was detected that displayed a difference in FC between the patient and healthy groups. The regions of this cluster include the left superior frontal (dorsolateral, orbital part), left middle frontal, middle frontal (left and right orbital part), left anterior cingulate and paracingulate, hippocampus (left and right), Cuneus (left and right), right thalamus, middle temporal (left and right), temporal pole: middle temporal (left and right) and inferior temporal (left and right). FC alterations in some of these regions can affect social interaction, memory, spatial processing, language

Table 1: Demographic information of the participants

Variable	ASD group	Healthy group	P
Age (years)	16.49 (7.63)	15.98 (6.31)	0.672
FIQ	108.96 (13.39)	108.84 (10.58)	0.663

Data are expressed as mean (SD). P -values were calculated by the Mann–Whitney U -test. FIQ=Full intelligence quotient; SD=Standard deviation; ASD=Autism spectrum disorder

acquisition, and cognitive processes. In Figure 1, the disease-related cluster of regions is depicted in light blue, and other areas are depicted in dark blue. Figure 2 shows the $-\log(p\text{-values})$ of the pairwise FC comparisons of 90 regions between the two groups. The regions in the figure are ordered according to their placement in the cluster. The FC comparisons of the cluster's regions had high P values, indicating the accurate detection of clustering by the ADSD model.

The FC of pairwise regions in the cluster was compared between the patient and healthy groups using the variance component model. The average correlation of all subjects within each of the two groups is depicted in Figure 3. The size and color of the circles are changed according to the correlation's value. Figure 4 shows the results of the analysis for each region's pair. There was a significant

difference between the two groups on 36 edges out of 17 (17 - 1)2 = 136. The middle temporal gyrus (MTG) had more communication than the other regions in the cluster. The largest difference between groups was -0.112 , which corresponding to the right middle temporal and right thalamus regions. Further details of the test results, including the estimated difference of the correlation between regions in the two groups and their P values, are presented in Table 2 (Further details on the full names of the regions are available in the appendix 1).

DISCUSSION

This study examined FC alterations in 294 autistic patients and 312 healthy individuals using the ADSD and the variance component model. The ADSD model detects a cluster of disease-related and biologically

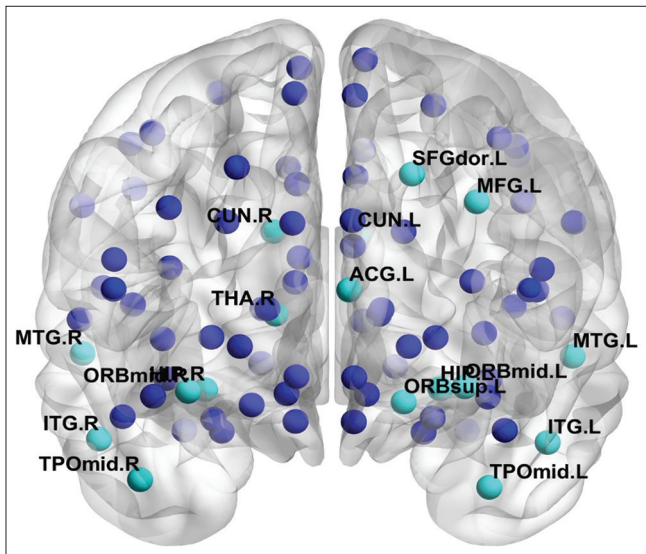


Figure 1: Disease-related regions (light blue circles) extraction by the adaptive dense subgraph discovery model

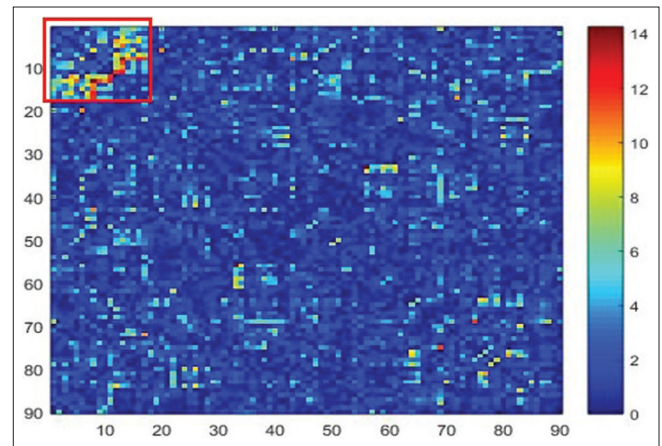


Figure 2: The $-\log(p\text{-values})$ of the pairwise functional connectivity comparisons of 90 regions between the two groups (The cluster extraction by the adaptive dense subgraph discovery model is shown in the red box)

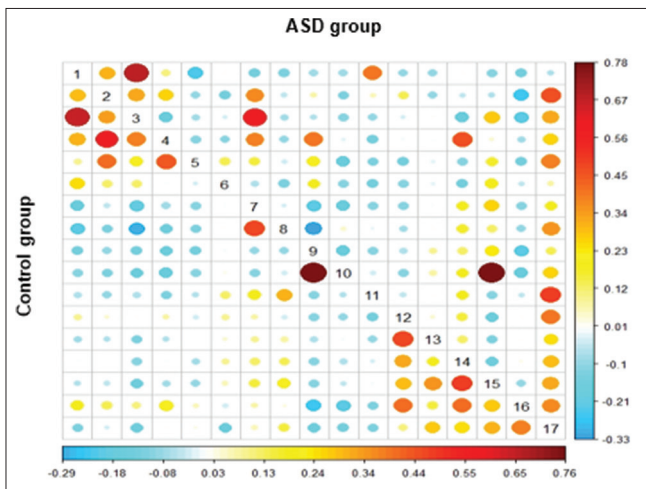


Figure 3: The average correlation of all subjects within each of the two groups. ASD: Autism spectrum disorder

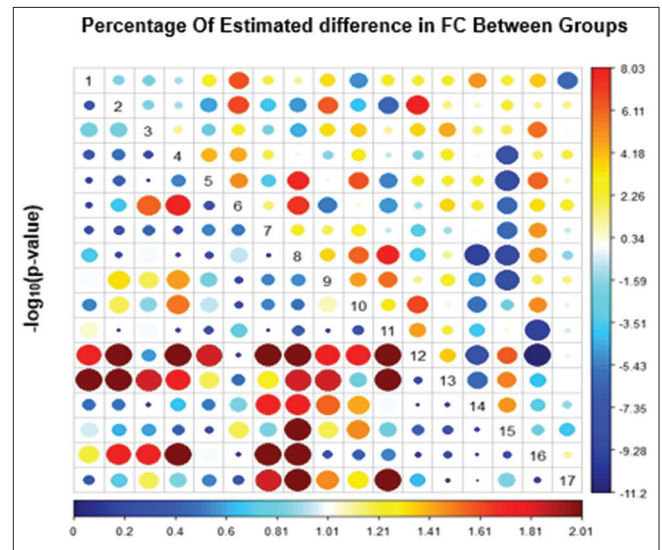


Figure 4: The results of the functional connectivity analysis for each regions pair between the two groups using the variance component model. FC: Functional connectivity

Table 2: Differentially expressed edges between the two groups by the variance component model

Index	Different expressed edges		P ^a	Estimated difference ^b
1	SFGdor.L	↔ MTG.L	0.019	0.065
2	SFGdor.L	↔ MTG.R	0.009	0.068
3	ORBsup.L	↔ CUN.L	0.049	-0.048
4	ORBsup.L	↔ MTG.L	0.009	0.076
5	ORBsup.L	↔ MTG.R	0.009	0.073
6	ORBsup.L	↔ ITG.L	0.019	0.063
7	MFG.L	↔ ACG.L	0.027	-0.054
8	MFG.L	↔ MTG.R	0.014	0.065
9	MFG.L	↔ ITG.L	0.019	0.060
10	ORBmid.L	↔ ACG.L	0.019	-0.061
11	ORBmid.L	↔ CUN.L	0.036	-0.051
12	ORBmid.L	↔ CUN.R	0.030	-0.048
13	ORBmid.L	↔ MTG.L	0.009	0.080
14	ORBmid.L	↔ MTG.R	0.018	0.058
15	ORBmid.L	↔ ITG.L	0.009	0.079
16	ORBmid.R	↔ MTG.L	0.014	0.067
17	HIP.L	↔ MTG.L	0.009	-0.094
18	HIP.L	↔ TPOmid.L	0.019	-0.056
19	HIP.L	↔ ITG.L	0.009	-0.082
20	HIP.L	↔ ITG.R	0.014	-0.060
21	HIP.R	↔ MTG.L	0.009	-0.078
22	HIP.R	↔ MTG.R	0.014	-0.087
23	HIP.R	↔ TPOmid.L	0.018	-0.062
24	HIP.R	↔ TPOmid.R	0.009	-0.062
25	HIP.R	↔ ITG.L	0.009	-0.089
26	HIP.R	↔ ITG.R	0.009	-0.085
27	CUN.L	↔ MTG.L	0.018	0.063
28	CUN.L	↔ MTG.R	0.014	0.055
29	CUN.L	↔ TPOmid.L	0.027	0.051
30	CUN.L	↔ ITG.R	0.032	0.058
31	CUN.R	↔ MTG.L	0.019	0.061
32	CUN.R	↔ TPOmid.L	0.038	0.051
33	CUN.R	↔ TPOmid.R	0.032	0.050
34	THA.R	↔ MTG.L	0.009	-0.095
35	THA.R	↔ MTG.R	0.009	-0.112
36	THA.R	↔ ITG.R	0.009	-0.061

^aP-values were calculated by the variance component model, ^bEstimated difference of the correlation between regions in patient and healthy individuals. Further details on the full names of the regions are available in the appendix. Parameter estimation of the edges between regions in the patient and healthy group

interpretable regions by minimizing false positive and false negative noises. According to the result of this model, a disease-related cluster of 17 regions was identified, such as the hippocampus, cuneus, and inferior temporal. Connectivity alterations in these regions can affect social interaction, memory, spatial processing, and language acquisition.^[14-16] In this regard, Chen *et al.* used advanced statistical methods to study the brain connectivity subnetworks in autism patients. Common areas in the subnetworks with the ADSD model included the middle frontal (left orbital part), anterior cingulate and paracingulate (left), and temporal pole: middle temporal and right inferior temporal.^[17] Another study in patients

with autism reported connectivity changes in the right thalamus, middle temporal, and right inferior temporal.^[18] According to Pascual-Belda *et al.*, FC changes influence the temporal and frontal lobe, as well as the limbic system.^[19]

The variance component model is used to compare the FC of regions pairwise in the cluster between two groups by considering the main features of FC data, including temporal autocorrelation and subject heterogeneity. In this model, the connectivity of 36 region pairs was significantly different between the patient and healthy groups. Compared to other regions, the MTG displayed more communication. The largest difference between groups is also related to the right middle temporal region and the right thalamus. The MTG region is involved in language and semantic memory processing, which can be related to the behaviors of people with ASD.^[20] Xu *et al.* presented that altered MTG subregions in children and adults with ASD were linked to social cognition and language.^[21] Another study on brain connectivity in people with ASD showed that the parahippocampus and thalamus can be diagnostic biomarkers for autism.^[22]

The connectivity of the left anterior cingulate and paracingulate (ACG. L) with the left middle frontal and left middle frontal (orbital part) regions was significantly different between the two groups. The connectivity altered of ACG. L, as regions of the default mode network (DMN), can affect cognitive processes. In this regard, Kennedy and Courchesne showed decreased activity of the anterior cingulate cortex in patients with ASD.^[23] In people with ASD, increased connectivity in the brain regions of the DMN may be associated with social impairment symptoms.^[24] In addition, various investigations have identified connectivity alternations of DMN regions in patients with ASD.^[25-28]

CONCLUSION

To accurately estimate the FC structure associated with phenotypes of neurological diseases, it is critical to use appropriate statistical models. In this study, advanced graph-based models were employed to investigate changes in communication patterns across different brain regions in autistic patients. The results showed functional relationship alterations in patients with autism compared to healthy individuals, indicating the disease's effects on the brain connectivity network.

Financial support and sponsorship

Nil.

Conflicts of interest

There are no conflicts of interest.

REFERENCES

1. Maenner MJ, Shaw KA, Baio J, Washington A, Patrick M, *et al.* Prevalence of autism spectrum disorder among children aged 8 years – Autism and developmental disabilities monitoring network, 11 sites, United States, 2016. *MMWR Surveill Summ* 2020;69:1-12.
2. Chaste P, Leboyer M. Autism risk factors: Genes, environment, and gene-environment interactions. *Dialogues Clin Neurosci* 2012;14:281-92.
3. Chen L, Chen Y, Zheng H, Zhang B, Wang F, Fang J, *et al.* Changes in the topological organization of the default mode network in autism spectrum disorder. *Brain Imaging Behav* 2021;15:1058-67.
4. Greicius M. Resting-state functional connectivity in neuropsychiatric disorders. *Curr Opin Neurol* 2008;21:424-30.
5. Moore V, Goodson S. How well does early diagnosis of autism stand the test of time? Follow-up study of children assessed for autism at age 2 and development of an early diagnostic service. *Autism* 2003;7:47-63.
6. Fernell E, Eriksson MA, Gillberg C. Early diagnosis of autism and impact on prognosis: A narrative review. *Clin Epidemiol* 2013;5:33-43.
7. Lehmann BC, Henson RN, Geerligs L, Cam-Can, White SR. Characterising group-level brain connectivity: A framework using Bayesian exponential random graph models. *Neuroimage* 2021;225:117480.
8. Simpson SL, Moussa MN, Laurienti PJ. An exponential random graph modeling approach to creating group-based representative whole-brain connectivity networks. *Neuroimage* 2012;60:1117-26.
9. Zalesky A, Fornito A, Bullmore ET. Network-based statistic: Identifying differences in brain networks. *Neuroimage* 2010;53:1197-207.
10. Wu Q, Huang X, Culbreth AJ, Waltz JA, Hong LE, Chen S. Extracting brain disease-related connectome subgraphs by adaptive dense subgraph discovery. *Biometrics* 2022;78:1566-78.
11. Fiecas M, Cribben I, Bahktiari R, Cummine J. A variance components model for statistical inference on functional connectivity networks. *Neuroimage* 2017;149:256-66.
12. Craddock C, Benhajali Y, Chu C, Chouinard F, Evans A, Jakab A, *et al.* The neuro bureau preprocessing initiative: Open sharing of preprocessed neuroimaging data and derivatives. *Front Neuroinform* 2013.
13. Tzourio-Mazoyer N, Landeau B, Papathanassiou D, Crivello F, Etard O, Delcroix N, *et al.* Automated anatomical labeling of activations in SPM using a macroscopic anatomical parcellation of the MNI MRI single-subject brain. *Neuroimage* 2002;15:273-89.
14. Banker SM, Gu X, Schiller D, Foss-Feig JH. Hippocampal contributions to social and cognitive deficits in autism spectrum disorder. *Trends Neurosci* 2021;44:793-807.
15. Rolls ET, Zhou Y, Cheng W, Gilson M, Deco G, Feng J. Effective connectivity in autism. *Autism Res* 2020;13:32-44.
16. Cai J, Hu X, Guo K, Yang P, Situ M, Huang Y. Increased left inferior temporal gyrus was found in both low function autism and high function autism. *Front Psychiatry* 2018;9:542.
17. Chen S, Xing Y, Kang J. Latent and abnormal functional connectivity circuits in autism spectrum disorder. *Front Neurosci* 2017;11:125.
18. Chen S, Kang J, Xing Y, Wang G. A parsimonious statistical method to detect groupwise differentially expressed functional connectivity networks. *Hum Brain Mapp* 2015;36:5196-206.
19. Pascual-Belda A, Díaz-Parra A, Moratal D. Evaluating functional connectivity alterations in autism spectrum disorder using network-based statistics. *Diagnostics (Basel)* 2018;8:51.
20. Onitsuka T, Shenton ME, Salisbury DF, Dickey CC, Kasai K, Toner SK, *et al.* Middle and inferior temporal gyrus gray matter volume abnormalities in chronic schizophrenia: An MRI study. *Am J Psychiatry* 2004;161:1603-11.
21. Xu J, Wang C, Xu Z, Li T, Chen F, Chen K, *et al.* Specific functional connectivity patterns of middle temporal gyrus subregions in children and adults with autism spectrum disorder. *Autism Res* 2020;13:410-22.
22. Yang X, Zhang N, Schrader P. A study of brain networks for autism spectrum disorder classification using resting-state functional connectivity. *Mach Learn Appl* 2022;8:100290.
23. Kennedy DP, Courchesne E. Functional abnormalities of the default network during self- and other-reflection in autism. *Soc Cogn Affect Neurosci* 2008;3:177-90.
24. Qin B, Wang L, Cai J, Li T, Zhang Y. Functional brain networks in preschool children with autism spectrum disorders. *Front Psychiatry* 2022;13:896388.
25. Cherkassky VL, Kana RK, Keller TA, Just MA. Functional connectivity in a baseline resting-state network in autism. *Neuroreport* 2006;17:1687-90.
26. Jung M, Kosaka H, Saito DN, Ishitobi M, Morita T, Inohara K, *et al.* Default mode network in young male adults with autism spectrum disorder: Relationship with autism spectrum traits. *Mol Autism* 2014;5:35.
27. Murdaugh DL, Shinkareva SV, Deshpande HR, Wang J, Pennick MR, Kana RK. Differential deactivation during mentalizing and classification of autism based on default mode network connectivity. *PLoS One* 2012;7:e50064.
28. Pourmotahari F, Doosti H, Borumandnia N, Tabatabaei SM, Alavi Majd H. Group-level comparison of brain connectivity networks. *BMC Med Res Methodol* 2022;22:273.

Appendix 1: Target anatomical areas according to the automated anatomical labeling atlas

Index	Regions	Abbreviations	Index	Regions	Abbreviations
1	Precentral_L	PreCG.L	46	Cuneus_R	CUN.R
2	Precentral_R	PreCG.R	47	Lingual_L	LING.L
3	Frontal_Sup_L	SFGdor.L	48	Lingual_R	LING.R
4	Frontal_Sup_R	SFGdor.R	49	Occipital_Sup_L	SOG.L
5	Frontal_Sup_Orb_L	ORBsup.L	50	Occipital_Sup_R	SOG.R
6	Frontal_Sup_Orb_R	ORBsup.R	51	Occipital_Mid_L	MOG.L
7	Frontal_Mid_L	MFG.L	52	Occipital_Mid_R	MOG.R
8	Frontal_Mid_R	MFG.R	53	Occipital_Inf_L	IOG.L
9	Frontal_Mid_Orb_L	ORBmid.L	54	Occipital_Inf_R	IOG.R
10	Frontal_Mid_Orb_R	ORBmid.R	55	Fusiform_L	FFG.L
11	Frontal_Inf_Oper_L	IFGoperc.L	56	Fusiform_R	FFG.R
12	Frontal_Inf_Oper_R	IFGoperc.R	57	Postcentral_L	PoCG.L
13	Frontal_Inf_Tri_L	IFGtriang.L	58	Postcentral_R	PoCG.R
14	Frontal_Inf_Tri_R	IFGtriang.R	59	Parietal_Sup_L	SPG.L
15	Frontal_Inf_Orb_L	ORBinf.L	60	Parietal_Sup_R	SPG.R
16	Frontal_Inf_Orb_R	ORBinf.R	61	Parietal_Inf_L	IPL.L
17	Rolandic_Oper_L	ROL.L	62	Parietal_Inf_R	IPL.R
18	Rolandic_Oper_R	ROL.R	63	SupraMarginal_L	SMG.L
19	Supp_Motor_Area_L	SMA.L	64	SupraMarginal_R	SMG.R
20	Supp_Motor_Area_R	SMA.R	65	Angular_L	ANG.L
21	Olfactory_L	OLF.L	66	Angular_R	ANG.R
22	Olfactory_R	OLF.R	67	Precuneus_L	PCUN.L
23	Frontal_Sup_Medial_L	SFGmed.L	68	Precuneus_R	PCUN.R
24	Frontal_Sup_Medial_R	SFGmed.R	69	Paracentral_Lobule_L	PCL.L
25	Frontal_Mid_Orb_L	ORBsupmed.L	70	Paracentral_Lobule_R	PCL.R
26	Frontal_Mid_Orb_R	ORBsupmed.R	71	Caudate_L	CAU.L
27	Rectus_L	REC.L	72	Caudate_R	CAU.R
28	Rectus_R	REC.R	73	Putamen_L	PUT.L
29	Insula_L	INS.L	74	Putamen_R	PUT.R
30	Insula_R	INS.R	75	Pallidum_L	PAL.L
31	Cingulum_Ant_L	ACG.L	76	Pallidum_R	PAL.R
32	Cingulum_Ant_R	ACG.R	77	Thalamus_L	THA.L
33	Cingulum_Mid_L	DCG.L	78	Thalamus_R	THA.R
34	Cingulum_Mid_R	DCG.R	79	Heschl_L	HES.L
35	Cingulum_Post_L	PCG.L	80	Heschl_R	HES.R
36	Cingulum_Post_R	PCG.R	81	Temporal_Sup_L	STG.L
37	Hippocampus_L	HIP.L	82	Temporal_Sup_R	STG.R
38	Hippocampus_R	HIP.R	83	Temporal_Pole_Sup_L	TPOsup.L
39	ParaHippocampal_L	PHG.L	84	Temporal_Pole_Sup_R	TPOsup.R
40	ParaHippocampal_R	PHG.R	85	Temporal_Mid_L	MTG.L
41	Amygdala_L	AMYG.L	86	Temporal_Mid_R	MTG.R
42	Amygdala_R	AMYG.R	87	Temporal_Pole_Mid_L	TPOmid.L
43	Calcarine_L	CAL.L	88	Temporal_Pole_Mid_R	TPOmid.R
44	Calcarine_R	CAL.R	89	Temporal_Inf_L	ITG.L
45	Cuneus_L	CUN.L	90	Temporal_Inf_R	ITG.R

Downloaded from <http://journals.lww.com/jrms> by BhDMf5ePHkav1zEoum1tQIN4a+kJLhEZgbsIHo4XMI0hCQwCt1AW nYQplIqH7D333D00dRy7TVSFI4C3V4OA/vpDDa8K2+Ya6H515KE= on 02/04/2024